Atmospheric Environment 85 (2014) 161–168

Contents lists available at ScienceDirect

Atmospheric Environment

journal homepage: www.elsevier.com/locate/atmosenv

Inter-seasonal variability in size-resolved CCN properties at Kanpur, India

Deepika Bhattu, Sachchida Nand Tripathi*

Department of Civil Engineering, Indian Institute of Technology Kanpur, Uttar Pradesh 208016, India

HIGHLIGHTS

- Size-and-time averaged κ (0.16) over 3 seasons shows dominance of organics.
- Despite of less κ, higher CCN/CN in spring is due to shifting of mode diameter.
- Increase in κ with particle diameter shows chemical composition vary with size.
- Among all seasons, particles are found to be most hygroscopic in summer.
- CCN prediction is more sensitive to κ in monsoon compared to other seasons.

ARTICLE INFO

Article history:
Received 9 October 2013
Received in revised form
5 December 2013
Accepted 11 December 2013

Keywords:
Cloud condensation nuclei
Hygroscopicity
Activation
Aitken mode
Accumulation mode

ABSTRACT

We present properties of size-resolved cloud condensation nuclei (CCN) over the central Indo-Gangetic Basin (IGB) station, Kanpur, India. The measurements were done during three different seasons: spring, summer and monsoon in 2012. Size-resolved CCN efficiency spectra (20–280 nm), measured at 0.2–1% supersaturation (*SS*), resulted in an average activation diameter (D_a) of 148–45 nm. The activation diameter was found to be maximum in spring followed by monsoon and summer at all *SS* except at *SS* = 1%. The size-averaged hygroscopicity (κ) of CCN-active particles for all *SS* was found to be 0.11 ± 0.03, 0.24 ± 0.13 and 0.14 ± 0.06 in spring, summer, and monsoon, respectively. κ increased with increasing particle diameter, suggesting change in chemical composition with size which further leads to change in CCN activity. In comparison to summer and monsoon, despite the presence of lower κ in spring, the higher activation fraction in Aitken mode is observed due to the shift of CN size distribution towards larger diameter. κ is observed to be lower in first half of the day (0900–1400 h) for *SS* = 0.2–0.5% due to relatively less photochemical activity compared to second half of the day. Size-and-time averaged κ value over all three seasons (0.16 ± 0.08) suggests dominance of organic species, as reported in previous studies.

1. Introduction

Changes in aerosol properties may also lead to higher cloud droplet concentration and smaller droplet size, thus increased cloud reflectivity (Twomey, 1974; Zhang et al., 2011) and decreased precipitation (Albrecht, 1989) in shallow and short lived clouds (Rosenfeld et al., 2008). This is known as the aerosol indirect effect and is the largest source of uncertainty in climate change (IPCC et al., 2007). Various past studies have addressed the role of anthropogenic aerosols in alteration of cloud microphysical processes and radiative properties (Hudson and Yum, 2002; Lohmann and Feichter, 2005 and references therein). The aerosol particles act as cloud condensation nuclei (CCN), thus enabling the formation of cloud droplets (0.1–10 μm) when the ambient partial pressure of water vapour (ρ_w) is greater than the saturation vapour pressure (ρ°_w) resulting in a supersaturated condition (Ruehl et al., 2008). Several initiatives have been taken to assess the CCN activity of ambient aerosols over the last two decades, but the need for global data is still not fulfilled (Kulmala et al., 2004). Thus, accurate prediction of global distribution of CCN is essential to improve our understanding of aerosol–cloud–climate interactions (IPCC et al., 2007), and to make reliable prediction of future climate forcing. The ultimate aim is to include the effects of these interactions in the meteorological models through various parameterization schemes (Rose et al., 2010).

One of the challenging tasks is to evaluate the relative importance of aerosol size distribution, chemical composition, mixing state, dissolution behaviour inside the droplet, and surface tension

* Corresponding author.
E-mail addresses: snt@iitk.ac.in, tripathi_sn@hotmail.com (S.N. Tripathi).

1352-2310/$ – see front matter © 2013 Elsevier Ltd. All rights reserved.
http://dx.doi.org/10.1016/j.atmosenv.2013.12.016

in the prediction of CCN concentration (Pruppacher and Klett, 1997). Several researchers have shown the primary role of total aerosol (CN) size distribution and number concentration in establishing the tendency of aerosols to act as CCN at atmospherically prevailing conditions (Dusek et al., 2006; Sihto et al., 2011). Recent model studies have shown that for regions with higher particle concentration and internally-mixed aerosols, chemical composition is an important controlling factor influencing cloud droplet number concentration (Ervens et al., 2005). Previous size-resolved CCN activation laboratory studies were based on the behaviour of known chemical compounds, such as water soluble organic and inorganic compounds separately, and their mixtures. The formation process and solubility of an organic particle, affecting its CCN activation behaviour were also investigated (Rissman et al., 2007 and references therein). However, in recent years, the size-resolved CCN activity of ambient aerosols has gained much more attention compared to laboratory generated aerosols (Rose et al., 2010; Gunthe et al., 2009; Cerully et al., 2011). Several field studies have been done in tropical (Gunthe et al., 2009), coniferous (Levin et al., 2012), and boreal forests (Cerully et al., 2011; Sihto et al., 2011) to understand the effect of biogenic organic aerosols on hygroscopicity. During AMAZE-2008 campaign in central Amazonia, Aitken mode ($D = 50–90$ nm; $\kappa = 0.1$) particles were found to be less hygroscopic than accumulation mode ($D = 100–200$ nm; $\kappa = 0.2$) particles, exhibiting the possibility of presence of secondary organic aerosols in the Aitken mode particles (Gunthe et al., 2009). It has been also found that hygroscopicity is lower for fresh biomass burning aerosols, compared to aged ones with varying κ distributions (Petters et al., 2009). Size-segregated measurements at Cape Hedo, Japan, showed high particle hygroscopicity due to internally-mixed nature of sulphate rich aerosols (Mochida et al., 2010). Bougiatioti et al. (2011) found that particles of less than 40 nm diameter were more hygroscopic than larger ones (80 nm). They also observed a strong diurnal variation in the particles of diameter less than 80 nm because of the photochemical activity, and volatilization of less hygroscopic species. These measurements provide a unique perspective on chemical distribution of atmospheric species, and processes affecting CCN activity (Asmi et al., 2012).

Size-resolved CCN measurements are increasingly becoming common practice for decoupling the effect of size and chemical composition on CCN activity, and characterizing chemical ageing and mixing state of aerosols (Frank et al., 2006). The assessment of the effect of aerosol chemical composition on CCN activity using a single hygroscopicity parameter (κ) has been demonstrated in the past few years (Petters and Kreidenweis, 2007). It can quantitatively measure the ability of aerosols to uptake water vapours under atmospheric conditions, and their CCN activity. Several studies have documented the application of κ in predicting CCN concentration in model simulations (Moore et al., 2012) and field measurements (Moore et al., 2011; Sihto et al., 2011). Several authors have reported the hygroscopic properties of aerosols using hygroscopicity tandem differential mobility analyzer (HTDMA) under sub-saturated conditions. These properties can be used to infer the CCN activity at various saturation levels (Rissler et al., 2004; Vestin et al., 2007). It was found that the presence of high organic fraction, either soluble or insoluble, is responsible for different hygroscopic properties under sub-saturated and supersaturated regimes (Lance et al., 2012). Also, the effect of mixing state of aerosols has been seen in the HTDMA and CCNc-derived critical diameters (Sihto et al., 2011). It was found that the assumption of internally-mixed aerosols did not make much difference between the two methods. It was observed that the particles were mainly composed of organics along with more hygroscopic species like, inorganics. It has also been observed that oxygen to carbon (O:C) ratio of secondary organic aerosols (SOA) has both linear (Chang et al., 2010) and non-linear (Massoli et al., 2010) relationship with HTDMA and CCNc-derived κ value. Carrico et al. (2010) also attempted to predict κ from filter based particulate matter mass ($PM_{2.5}$) measurements during laboratory investigations. They employed simple mixing rule (Petters and Kreidenweis, 2007) and simplified assumptions of κ and density for their four-component model. Both the measured (HTDMA) and predicted κ values were found to be in reasonable agreement (Carrico et al., 2010).

Although, several studies have reported size-resolved CCN measurements (e.g. Gunthe et al., 2009, 2011; Rose et al., 2010; Bougiatioti et al., 2011), and long term variation in hygroscopicity parameter and CCN concentration (Levin et al., 2012; Asmi et al., 2012; Fors et al., 2011; Kammermann et al., 2010) worldwide, there are currently no reports from India. The ground-based seasonal CCN measurements and their closure analysis using size–invariant chemical composition have been previously looked into from Indian region (Patidar et al., 2012). In addition, the closure results from in-situ aircraft measurements for 6 flight sorties were also obtained during Indian Continental Tropical Convergence Zone (CTCZ) campaign (Srivastava et al., 2013). To the best of our knowledge, this is the first study from India reporting the seasonal variation of size-resolved CCN activity in terms of single hygroscopicity parameter, as a function of dry particle diameter and critical water vapour supersaturation. The objective is to develop an understanding of the relative contribution of different aerosol types like, dust, organic and inorganic to CCN activity in different seasons. This study also compares some of its results with the field measurements at other continental regions.

2. Experimental details

2.1. Sampling site and meteorological conditions

The measurements were done at the first floor (~5 m above ground) of the Western Laboratory of the Indian Institute of Technology, Kanpur (80.3 °E, 26.5 °N, 142 m above mean sea level). Data was collected over three seasons in 2012: spring (Feb 28–March 7), summer (May 28–June 14) and monsoon (Aug 24–Aug 30). Kanpur is located in the central part of the Indo-Gangetic Basin (IGB) and is representative of general characteristics of aerosols over IGB, Northern India. This urban sampling site is ~15 km upwind of the Kanpur city (Ram et al., 2010). The potential sources of aerosols are combustion of fossil fuels, bio-fuels, and other anthropogenic sources like thermal power plant and vehicular emission (Jai Devi et al., 2011; Dey and Tripathi, 2008). Spring and early summer are influenced by westerly and north-westerly winds bringing dust from Thar desert in Rajasthan, and semi-arid regions of Middle-East (Ram et al., 2010; Mishra et al., 2008). The meteorological parameters recorded during the sampling period were: relative humidity (RH) and temperature (Vaisala, Inc. Humicap, HMT337, accuracy of 1% for RH < 90%) (Table 1). Wind speed is taken from NCEP Reanalysis data. Back trajectory analysis done using HYSPLIT model (Draxler and Hess, 1997) using GDAS (Global Data Assimilation

Table 1
Meteorological parameters: Average (arithmetic mean ± 1 standard deviation) wind speed, RH and temperature in different seasons, viz., spring, summer and monsoon.

Seasons	Wind speed (ms^{-1})	Relative humidity (%)	Temperature (°C)
Spring (March)	2.68 ± 1.65	36.34 ± 10.46	23.03 ± 4.04
Summer (May–June)	3.51 ± 1.41	18.77 ± 7.34	40.18 ± 3.50
Monsoon (August)	2.25 ± 1.42	70.17 ± 10.32	29.90 ± 2.33

System) meteorological data shows that the transport pathway of air mass affecting the sampling site varies with the season.

2.2. Instrumentation and measurement details

Ambient aerosol particles, passed through silica-gel diffusional dryer (RH<30%), were imparted charge equilibrium through Kr85 bipolar charger, and were classified with the Differential Mobility Analyser (DMA; TSI 3081; Sample flow rate = 0.8 lpm and sheath flow rate = 8 lpm). Particles were classified on the basis of their electrical mobility in the DMA. These size-selected particles were counted by Droplet Measurement Technologies Continuous-Flow Streamwise Thermal-Gradient CCN counter (CCN-100; Roberts and Nenes, 2005; Flow rate = 0.5 lpm; Sheath to aerosol ratio = 10:1) and Condensation Particle Counter (CPC; TSI 3775; Flow rate = 0.3 lpm). Prior to the start of each sampling period, calibration was done using monodisperse ammonium sulphate (purity > 99%, Fischer Scientific) particles for five different ΔT ranging from 3 K–16 K in order to calculate effective supersaturation, SS_{eff} as shown in Fig. S1 (Rose et al., 2008; Patidar et al., 2012). To obtain size-resolved CCN activation spectra at five selected supersaturation levels (0.2%, 0.3%, 0.5%, 0.8%, 1.0%), 15-20 different particle diameter (2 min each) were selected in the range of 20–280 nm depending on the *SS* chosen. In the middle of sampling period of each supersaturation, aerosol size distribution (after every 10–12 min) was obtained from SMPS (Scanning Mobility Particle Sizer, Sheath to aerosol ratio = 10:1). One complete set of five different supersaturations was covered in 320 min that include sufficient adjustment time between two supersaturation levels. First 60 s of every 2 min data set is discarded, and the data integration time was kept at 60 s that included all the data points during that period. Total 240 (48 spectra at 5 *SS*) size-resolved CCN efficiency spectra were obtained: March (7), May–June (30) and August (11) with few gaps due to rain in August, and instrument related problems in spring. O_3 and CO concentrations was also measured during the sampling period at aerosol monitoring station, located 400 m away from the sampling site to the north-east direction inside the campus. The air mass sampled during one complete set of experiment showed ~20–30% variability showing its homogeneous nature.

2.3. Methodology

Corrections for multiply-charged particles (Frank et al., 2006) and DMA transfer function (Rose et al., 2008) were applied to all size-resolved CCN efficiency spectra. For multiple charge correction, the aerosol size distribution measured by SMPS between supersaturation cycles is used with an assumption that the size distribution did not vary significantly over a short duration (~10–12 min). This assumption is based on our 5-year SMPS size distribution statistical analysis (Kanawade et al., in preparation). Baxla et al. (2009) found that seasonal variation in aerosol size distribution is more pronounced compared to diurnal variation, hence the assumption is valid for the conditions prevailing in Kanpur. The correction for CCN and CPC counting inefficiency was not required as for pure ammonium sulphate particles, the CCN/CN ratio reached unity for all ΔT considered. Besides, the correction for *SS* depletion was not applied because the total CCN concentration never reached the threshold value of 5000 particles cm^{-3} during the sampling period (Lathem and Nenes, 2011). The measured CCN efficiency spectrum was fitted using Equation (1) (Rose et al., 2008)

$$f_{\mathrm{CCN/CN}} = a\left(1 + \mathrm{erf}\left(\frac{D - D_a}{\sigma_a\sqrt{2}}\right)\right) \quad (1)$$

The fit parameters, a and σ_a are half of the maximum activated fraction (MAF = $2a$), and standard deviation of the fit, respectively. D_a is the dry particle diameter at which CCN/CN fraction reaches 50% of its maximum value. These parameters correspond to properties of CCN active particles. MAF < 1 suggests the external mixing of CCN active species with CCN inactive species from D_a to $D_{\max}$. σ_a depicts the width of chemical distribution of CCN active particles. Under ideal conditions, the heterogeneity parameter (σ_a/D_a) for single component system should be nearly zero. However, for the calibration aerosols (ammonium sulphate), it is found to be ~3% which could be due to particles morphological properties and DMA transfer function effects, and changes in the supersaturation conditions of the system (Gunthe et al., 2009; Rose et al., 2010).

To parameterize the effect of chemical composition on CCN activity of aerosols, the hygroscopicity parameter, κ, was calculated using Equation (2) below. It is worth mentioning that κ accounts for not only the effect of solute on water activity, but also changes in surface tension. It is based on Köhler theory relating critical dry particle diameter to critical water vapour supersaturation (Petters and Kreidenweis, 2007; Rose et al., 2010).

$$s = \frac{D_{\mathrm{wet}}^3 - D_a^3}{D_{\mathrm{wet}}^3 - D_a^3(1-\kappa)}\exp\left(\frac{4\sigma_{\mathrm{sol}}M_w}{\mathrm{RT}\rho_w D_{\mathrm{wet}}}\right) \quad (2)$$

Here, D_{wet} is the droplet diameter corresponding to particular saturation ratio, S=(1 + *SS*/100%). κ is calculated for T = 298.15 K, σ_{sol} = 0.072 J m^{-2}, R = 8.315 J K^{-1} mol^{-1}, ρ_w = 997.1 kg m^{-3} and M_w = 0.018015 kg mol^{-1}. κ obtained using D_a and *SS* tells us about the average hygroscopicity of CCN active particles in that particular size range around D_a (Gunthe et al., 2009). The procedure given by Rose et al. (2010) was used to calculate κ for all pairs of supersaturation and activation diameter. D_a was obtained from the Cumulative Gaussian Distribution function (CDF) fit of measured CCN/CN spectrum by using Equation (1). Both the parameters D_{wet} and κ were varied until the difference between calculated saturation ratio (S in Equation (2)) and the measured saturation ratio ($S_{\mathrm{measured}} = 1 + SS_{\mathrm{measured}}/100\%$) approached a minimum value. In addition, CCN size distribution (dCCN/d*logD*) is calculated by multiplying the seasonally averaged CCN/CN spectra with the seasonally averaged CN size distribution (dCN/d*logD*) obtained from the SMPS. Seasonally averaged total CCN concentration is calculated by integrating the calculated CCN size distribution.

3. Results and discussion

3.1. Inter-seasonal variability

The average CCN efficiency spectra for three different seasons: spring, summer and monsoon are shown in Fig. 1. The activation diameter increased with decreasing *SS*, and was found to be largest in spring followed by monsoon and summer at all *SS* except at *SS* = 1%. It is also observed that nearly 93–100% of the particles with diameter greater than the activation diameter were CCN-active (Table 2). At lower *SS* = 0.2%, the fraction of externally mixed CCN-inactive particles, averaged over the range of D_a to $D_{\max}$, was found to be maximum in summer (~0.07). At intermediate (*SS* = 0.3–0.5%) and higher (*SS* = 0.8–1.0%) supersaturation, MAF increased to maximum of 1 showing lesser participation of CCN-inactive species at these *SS* levels. The average heterogeneity parameter (σ_a/D_a) showed less seasonal variation (σ_a/D_a = 0.18–0.2) for accumulation mode particles except in spring, compared for Aitken mode (D < 100 nm) particles (σ_a/D_a = 0.11–0.35). Also, the seasonally averaged κ derived from the D_a, obtained through CDF fit of the measured CCN efficiency spectra, ranges between 0.03 and 0.42 during the measurement period. This seasonal variation in κ

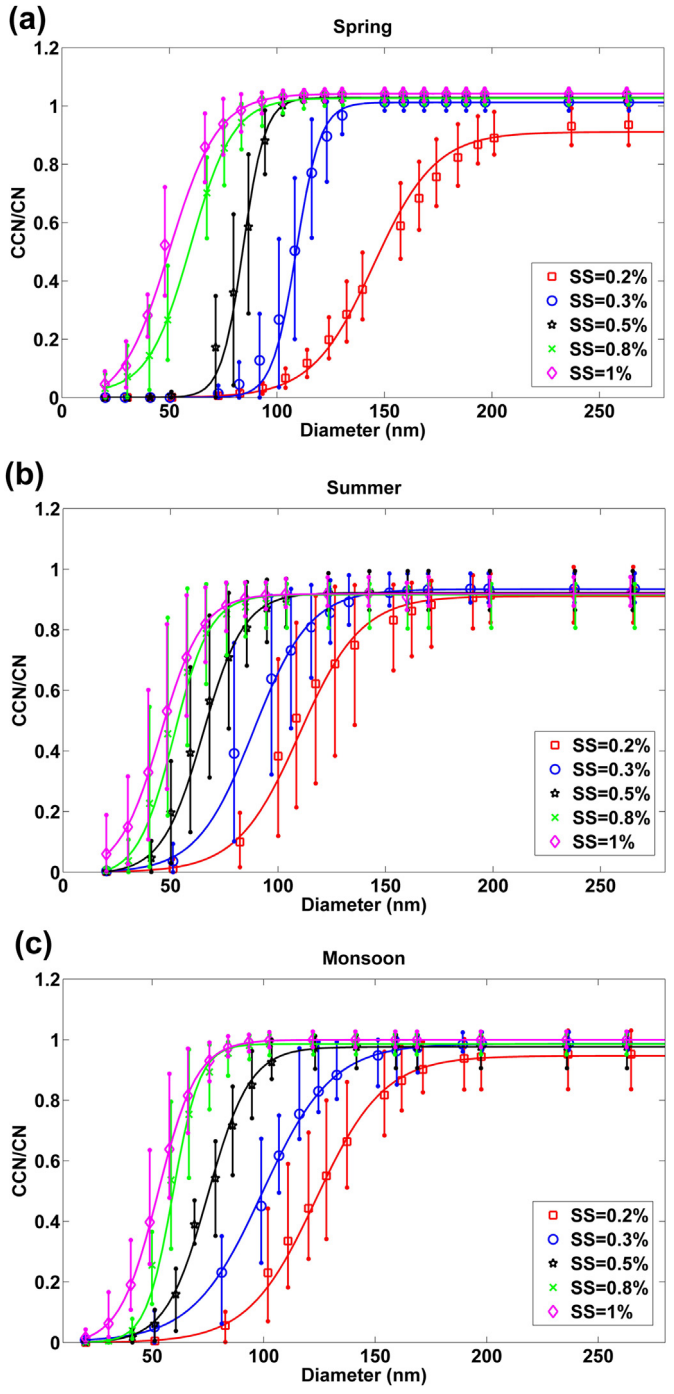

Fig. 1. Averaged size-resolved CCN efficiency spectra at 5 different water vapour supersaturations (SS = 0.2%, 0.3%, 0.5%, 0.8%, 1.0%) for the three seasons studied in this work: (a) Spring, (b) Summer and (c) Monsoon. Each data point is the mean value obtained from the CDF fit to the measured CCN efficiency spectra corresponding to the particular mobility diameter, the solid lines are Cumulative Gaussian Distribution fit and error bar is the difference of upper and lower quartiles.

could be due to changes in chemical composition attributed to contrasting regional emission source strength, boundary layer dynamics and SOA formation (Ram et al., 2010, 2012). In summer, both the accumulation mode particles and Aitken mode particles were found to have maximum κ (0.29 and 0.22, respectively), followed by monsoon (0.20 and 0.12, respectively) and spring (0.11 and 0.10, respectively). Size and seasonal averaged κ was found to be 0.11, 0.24 and 0.14 for spring, summer and monsoon, respectively. According to past studies, higher WSOC/OC and OC/EC from biomass burning found in summer compared to lower OC/EC from fossil fuel explains the high κ values in summer (Ram et al., 2010, 2012). Same study also demonstrated the vehicular emission and mineral dust to be potential sources of aerosols during spring while mineral dust aerosols dominate in the summer. κ value increased with decrease in supersaturation during summer and monsoon indicating size dependent chemical composition of the aerosols (Levin et al., 2012; Rose et al., 2010; Gunthe et al., 2009). However, Kim et al. (2011) and Bougiatioti et al. (2011) found exactly opposite to these findings at two remote islands and during FAME07, and attributed it to the photochemical activity and further condensation of low volatility products.

Table 2
Average (arithmetic mean ± 1 standard deviation) CDF fit parameters (D_a, MAF, σ_a, σ_a/D_a, κ) for the three seasons studied in this work: spring, summer and march. n is number of data points.

Spring: February–March (n = 7)					
SS (%)	D_a	MAF	σ_a	σ_a/D_a	κ
Accumulation mode					
0.2	148.54 ± 9.86	0.95 ± 0.06	29.42 ± 5.76	0.20 ± 0.03	0.10 ± 0.02
0.3	107.82 ± 10.09	1.01 ± 0.02	10.15 ± 4.24	0.09 ± 0.04	0.12 ± 0.03
Aitken mode					
0.5	83.27 ± 8.41	1.02 ± 0.01	8.79 ± 3.71	0.11 ± 0.05	0.10 ± 0.03
0.8	59.34 ± 7.31	1.02 ± 0.02	16.87 ± 6.38	0.29 ± 0.13	0.10 ± 0.04
1	50.19 ± 7.54	1.04 ± 0.02	16.39 ± 7.09	0.32 ± 0.12	0.11 ± 0.04
Summer: May–June (n = 26)					
Accumulation mode					
0.2	111.11 ± 19.68	0.93 ± 0.07	21.29 ± 13.56	0.18 ± 0.10	0.29 ± 0.13
Aitken mode					
0.3	87.92 ± 16.91	0.94 ± 0.05	17.93 ± 8,54	0.20 ± 0.10	0.26 ± 0.13
0.5	64.37 ± 11.56	0.92 ± 0.08	12.47 ± 5.78	0.18 ± 0.07	0.24 ± 0.13
0.8	50.31 ± 8.48	0.93 ± 0.06	10.11 ± 5.58	0.19 ± 0.09	0.20 ± 0.11
1	45.31 ± 9.34	0.92 ± 0.05	14.87 ± 7.17	0.35 ± 0.26	0.19 ± 0.15
Monsoon: August (n = 11)					
Accumulation mode					
0.2	123.28 ± 15.99	0.95 ± 0.09	23.42 ± 8.75	0.18 ± 0.06	0.20 ± 0.09
Aitken mode					
0.3	99.4419 ± 11.94	0.98 ± 0.05	24.96 ± 11.22	0.25 ± 0.12	0.16 ± 0.06
0.5	76.38 ± 5.89	0.97 ± 0.05	15.45 ± 3.84	0.20 ± 0.05	0.12 ± 0.09
0.8	58.60 ± 6.31	0.98 ± 0.03	9.95 ± 4.60	0.16 ± 0.07	0.11 ± 0.04
1	52.95 ± 6.24	0.99 ± 0.03	13.68 ± 4.18	0.26 ± 0.07	0.10 ± 0.04

3.2. κ variability

Seasonally averaged κ values with $\pm 1\sigma$, calculated from individual critical supersaturation and activation diameter are given in Table 2. There is a large seasonal variation in the κ value at all SS during summer and monsoon compared to spring, with maximum in summer showing more complex chemical composition. The variability in hygroscopicity of Aitken mode particles was found to be maximum in summer (κ = 0.07–0.44) due to the dominance of both highly hygroscopic and non-hygroscopic components (Fig. 2) followed by monsoon (κ = 0.07–0.23) and spring (κ = 0.07–0.16). Also, the accumulation mode particles showed higher variability (κ = 0.13–0.45) because air mass travelled from two different source origins viz., forest fire (in parts of Punjab and Haryana), and western part like desert (Middle East) and East Africa (Figs. S2 and S3). Previous studies have also reported the dominance of long range transported mineral dust aerosols during summer (Ram et al., 2010). Long range transport of insoluble species, like water insoluble organics, dust and black carbon (BC), cause ageing by changing their solubility and mixing state, thus affecting CCN activity (Fors et al., 2011). For SS = 0.2–0.3%, higher variation in κ was observed in monsoon (0.11–0.32) as compared to spring (0.08–

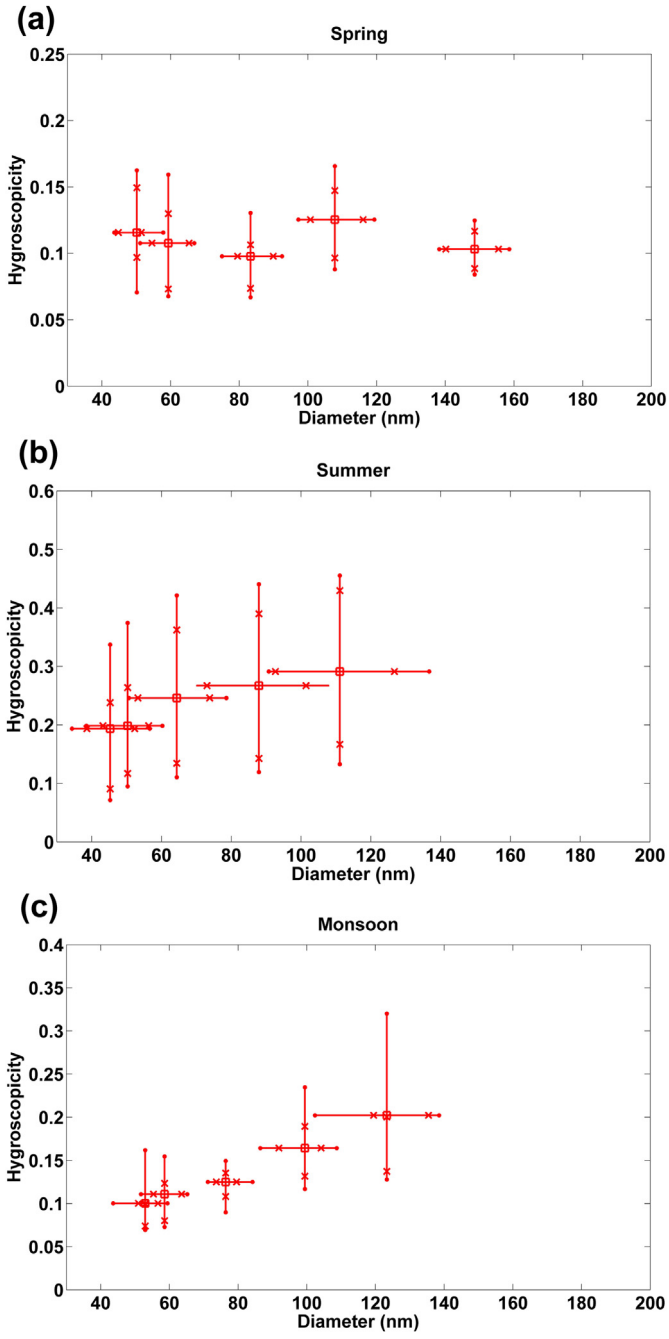

Fig. 2. Seasonal variation of κ values calculated at each measured supersaturation and activation diameter for (a) Spring, (b) Summer, and (c) Monsoon. The central rectangle shows mean, cross mark in *X* and *Y*-axis shows 25th–75th percentile and a dot at the end in both axis shows 10th and 90th percentile.

0.16) (Fig. 2). These results are in contrast to those obtained by Bougiatioti et al. (2011) and can be attributed to higher RH conditions, and larger variation in the wind speed that brought air mass from both land, and Arabian Sea and Bay of Bengal (Table 1). In monsoon, apart from following the same pattern of the Indian monsoon which brings the sea salt aerosols, air mass was also affected by the aerosols originated from land. Air mass during the spring season mainly originated in the Middle East, crossed Pakistan before entering Indian region, which shows that seasonal pattern is related to the source origin (Fig. S3; Ram et al., 2012). The presence of mixture of both highly hygroscopic species (like inorganic sulphate, sea salt) and less hygroscopic aerosol particles (like soil generated) travelling at different heights, can be a probable cause of κ variability.

The change in the hygroscopicity parameter within a day during different seasons is observed with κ value lower in the first half of the day (0900–1400 h) for $SS = 0.2–0.5\%$ due to less photochemical activity compared to second half of the day (Bougiatioti et al., 2011). However, for $SS = 0.8–1\%$, the species are found to be more hygroscopic in first half of the day because the second set of the experiment on the same day for same supersaturation was done in the declining phase (1800–2100 h) of the diurnal cycle of hygroscopicity. This variation in hygroscopicity decreased with increase in supersaturation (Fig. 2). It is important to note that summer season mostly had aged aerosols from burning events with significantly enhanced κ value due to high photochemical activity. The enhanced photochemical activity due to intense solar radiation during summer led to more oxidized species in the presence of strongly oxidizing agents such as H_2O_2 and O_3 which leads to increase in hygroscopic nature of aerosols (Fig. S4). Various field studies have used mixing rule to estimate the effect of organics on CCN activity (Gunthe et al., 2009; King et al., 2010). As we do not have chemical composition data during this study, we have used "hygroscopicity parameter (κ)" as an indicator of bulk chemical composition and explained it using previous chemical composition studies in Kanpur, IGB. Average κ value (0.24) indicates the presence of more water-soluble organic and inorganic species in summer compared to spring (0.11) and monsoon (0.14).

3.3. CCN and CN size distribution

In addition to aerosol hygroscopicity, seasonal changes were also observed in CCN and CN concentrations. CCN and CN size distribution for different seasons are presented in Fig. 3. The average CN size distributions for spring and summer were monomodal with maximum concentration at 200 nm and 168 nm, while in monsoon bimodal distribution was observed with first mode at 30 nm and second at 95 nm. As compared to monsoon and spring, summer has broader CN size distribution with large fraction of particles in size range greater than 168 nm because of the large growth rates due to enhanced photochemical activity. The number concentration of Aitken mode particles is lowest in spring while summer and monsoon are dominated by both Aitken and accumulation mode particles. In monsoon, only 26–36% of the total CN are activated at $SS = 0.2\%$ and 0.3% because modal diameter of the size distribution is less than or nearly equal to the activation diameter of CCN/CN efficiency spectra. In summer and spring both, modal diameter was always greater than activation diameter causing a major fraction (56–81%) to be activated at same supersaturation.

Average CCN concentration obtained from CCN size distribution increased with increase in *SS* in all seasons (Table 3). CCN/CN fractions at all supersaturations ($SS = 0.2–1\%$) in spring were largest compared to summer and monsoon CCN activation is a function of their hygroscopicity and dry particle size. Inspite of lower κ value in spring, maximum activated fraction is obtained because of the presence of smaller Aitken mode compared to summer and broader accumulation mode particles compared to monsoon (Fig. 3). This shows the significance of aerosol size distribution in estimating CCN concentration (Dusek et al., 2006; Levin et al., 2012). The sensitivity of CCN prediction to κ was also estimated by performing Köhler model calculations keeping size distribution constant. First case involved varying the κ (κ from the fitted measured CCN/CN efficiency spectra) while in the other κ was kept constant (0.3). The absolute average relative deviation ($|(CCN_{predicted}–CCN_{measured})|/CCN_{measured}$) was calculated for both

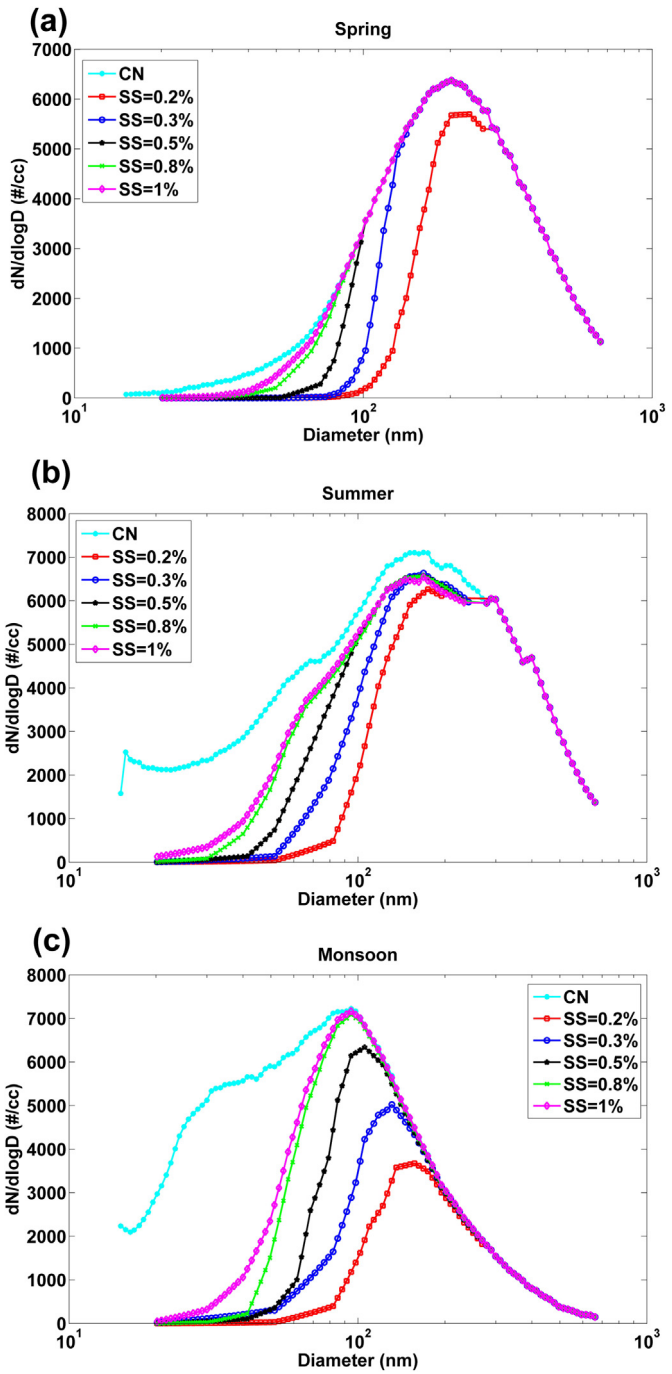

Fig. 3. Number size distribution of CN and CCN at SS = 0.2–1.0% averaged over (a) Spring, (b) Summer and (c) Monsoon. The size range of the CCN size distribution is limited by the size range of SMPS.

the cases in all seasons using the seasonally averaged size distributions. It increased with the decrease in SS in spring and monsoon (Table S1) explaining the importance of chemical composition at lower SS. Highest deviation is observed in monsoon due to the presence of higher concentration of Aitken mode particles for which chemical composition plays a major role in activation process. It has been observed that the total average relative deviation (considering all SS) is higher when κ is kept constant (~2–6 times). It has been observed that the relative deviation between $CCN_{predicted}$ and $CCN_{measured}$ is highest in monsoon followed by spring and summer, showing the significance of change in chemical composition. Thus, the variation in hygroscopicity of aerosols in different seasons cannot be overlooked in CCN prediction.

3.4. Comparison with other studies

It is important to note that very few studies show the seasonal variation of aerosol hygroscopicity, together with the CCN concentration, total aerosol concentration (CN) and aerosol size distribution (Kammermann et al., 2010; Levin et al., 2012). A long term study at remote location, Jungfraujoch, Switzerland showed that average chemical composition is sufficient to accurately predict CCN concentration (Jurányi et al., 2010, 2011). Another 11 months CCN study exhibited no seasonal variation in hygroscopicity from filter measurements and activation fraction, despite of the changes in seasonal chemical composition (Burkart et al., 2011, 2012). Similar study on seasonal variation of size resolved aerosol hygroscopicity has been carried out at a forest site located in Colorado (Levin et al., 2012). They found that accumulation mode aerosols were less hygroscopic in the summer compared to spring and fall seasons. In this study, inspite of lower κ value, higher activated fraction was found in spring which was due to the increase in geometric mean diameter (D_g). Moreover, κ values decreased with increase in supersaturation indicating change in chemical composition with particle size. Average κ value of 0.16 suggested the dominance of organics. Another similar kind of measurement at a pristine forest site pointed out that accumulation mode particles with κ = 0.2 were slightly more hygroscopic than Aitken mode (κ = 0.1). This is due to more ageing, cloud processing or larger inorganic fraction resulting in average κ = 0.3 that is representative of continental aerosols (Gunthe et al., 2009). κ values comparable to our study (κ = 0.07–0.42 at SS = 0.5–1%, and κ = 0.08–0.45 at SS = 0.2–0.3%) were also obtained at a regional site in the south of megacity of Beijing, China during the CAREBeijing-2006 campaign that showed κ value of ~0.25 and ~0.45 for Aitken and accumulation mode particles (Gunthe et al., 2011). Another study in southeastern China during PRIDE-PRD2006 campaign reported κ value of 0.1–0.5 (Rose et al., 2010). It was observed that κ decreased from 0.3 (campaign average) to 0.2 during local biomass burning event. The activated fraction obtained was ~6–~85% for SS = 0.068–1.27% comparable to pristine continental air.

Various other studies confirmed the presence of oxidized organics indicating increase in κ with O:C ratio (Cerully et al., 2011; Chang et al., 2010; Gunthe et al., 2011; Massoli et al., 2010 and references therein). Several other factors, such as photochemical oxidation of gas and particle phase chemical species, and condensation of low-volatility products, also add to aerosol hygroscopicity (Tritscher et al., 2011). Similar to other studies, the variation of κ with lower value in first half of the day is observed in this study, showing the dependence of aerosol hygroscopicity on their oxidation state (Cerully et al., 2011). Bougiatioti et al. (2011) found that

Table 3
Averaged total CN and CCN concentration and activated fraction (CCN/CN, in parenthesis) at SS = 0.2%, 0.3%, 0.5%, 0.8% and 1% for different seasons studied in this work: spring, summer and monsoon in complete SMPS size range, by fitting the CN size distribution by linear interpolation.

Season	Total CN (#/cc)	CCN (SS = 0.2%)	CCN (SS = 0.3%)	CCN (SS = 0.5%)	CCN (SS = 0.8%)	CCN (SS = 1%)
Spring (March)	4335	2686 (0.62)	3523 (0.81)	3899 (0.90)	4119 (0.95)	4187 (0.96)
Summer (May–June)	7107	3975 (0.56)	4572 (0.64)	5074 (0.71)	5432 (0.76)	5559 (0.78)
Monsoon (August)	6442	1659 (0.26)	2361 (0.36)	3014 (0.47)	3773 (0.58)	4095 (0.63)

smaller size particles ($D = 40$ nm) being less aged and more heterogeneous, exhibited more variation in hygroscopicity than bigger size particles ($D = 100$ nm). This indicates the presence of air masses from fresh anthropogenic emission. Variation in the mixing state of aerosols with more or less hygroscopic species also affects the activated fraction (Padró et al., 2012). Long range transport of aerosols make them internally mixed, hence making them more aged which also leads to higher activation fraction.

The assumption of uniform aerosol size distribution leads to much larger error (~60–70%) in predicting CCN concentration as compared to κ (Gunthe et al., 2009; Rose et al., 2010). It suggests that aerosol size distribution and number concentration are the major controlling factors, followed by chemical composition and hygroscopicity (Dusek et al., 2006). A recent study by Liu and Wang (2010) has also shown sensitivity analysis of aerosol indirect forcing to hygroscopicity parameter of organic aerosols that showed variation of 0.4 Wm^{-2} (−1.1 to −1.5 Wm^{-2}) with respect to control case of −1.3 Wm^{-2}. Thus an improved understanding of effect of organics on CCN activity in terms of hygroscopicity is required to decrease the current uncertainty in model calculations.

4. Conclusions

We have reported the first ever size-resolved CCN properties in different seasons at $SS = 0.2$–1.0% conducted at Kanpur, India. Over all, average κ value (size-and-time–averaged over all seasons) was found to be 0.16 ± 0.08 suggesting dominance of organic species. Seasonally averaged κ was 0.11 ± 0.03, 0.24 ± 0.13, 0.14 ± 0.06 in spring, summer and monsoon, respectively, showing air mass from different source origin (and/or mixed). A large seasonal variation in hygroscopicity is observed in particles with $D_p > 80$ nm (0.11 in spring, 0.28 in summer and 0.18 in monsoon) compared to $D_p < 80$ nm (0.10 in spring, 0.21 in summer and 0.11 in monsoon). The average κ value at lower supersaturation ($SS = 0.2\%$) dropped from 0.29 in summer to 0.20 in monsoon and 0.10 in spring. These higher values in summer are consistent with back trajectory analysis depicting the effect of long range transport of aerosols, sometimes accompanied by biomass burning. At lower activation diameter, significant variation in κ was not seen during spring and monsoon suggesting relatively lesser variation in chemical composition in Aitken mode particles. The diurnal variation in κ showed higher value in second half of the day in all seasons due to enhanced photochemical activity. In spring, particle size played significant role in CCN activation compared to chemical composition.

The sensitivity analysis of predicted CCN concentration to κ showed maximum deviation in monsoon with constant κ. So, our results suggest that seasonal variation in the critical diameter and κ should be taken into account for CCN prediction. These important inferences drawn from this study will assist in reducing the uncertainty in modelling CCN activation properties. However, a detailed chemical composition analysis is still required to better understand the effect of chemical composition on CCN activation properties.

Acknowledgement

This work is supported through a grant from Changing Water Cycle Programme of MoES, Govt. of India, and NERC, Govt. of U K. The authors acknowledge Dr. Vinod Tare for providing data of O_3, CO, NO_x and SO_2.We acknowledge the NOAA Air Resources Laboratory (ARL) for the provision of the HYSPLIT transport and dispersion model, and READY website (http://ready.arl.noaa.gov) used in this publication. Wind data used in this study was taken from National Center for Environmental Prediction (NCEP). We are thankful to Dr. V.P. Kanawade for his help in preparing the manuscript.

Appendix A. Supplementary data

Supplementary data related to this article can be found at http://dx.doi.org/10.1016/j.atmosenv.2013.12.016.

References

Albrecht, B.A., 1989. Aerosols, cloud microphysics, and fractional cloudiness. Science 245, 1227–1230.
Asmi, E., Freney, E., Hervo, M., Picard, D., Rose, C., Colomb, A., Sellegri, K., 2012. Aerosol cloud activation in summer and winter at puy-de-Dôme high altitude site in France. Atmos. Chem. Phys. 12, 11589–11607.
Baxla, S.P., Roy, A.A., Gupta, T., Tripathi, S.N., Bandyopadhyaya, R., 2009. Analysis of diurnal and seasonal variation of submicron outdoor aerosol mass and size distribution in a northern Indian city and its correlation to black carbon. Aerosol Air Qual. Res. 9, 458–469.
Bougiatioti, A., Nenes, A., Fountoukis, C., Kalivitis, N., Pandis, S.N., Mihalopoulos, N., 2011. Size-resolved CCN distributions and activation kinetics of aged continental and marine aerosol. Atmos. Chem. Phys. 11, 8791–8808.
Burkart, J., Steiner, G., Reischl, G., Hitzenberger, R., 2011. Long-term study of cloud condensation nuclei (CCN) activation of the atmospheric aerosol in Vienna. Atmos. Environ. 45 (32), 5751–5759.
Burkart, J., Hitzenberger, R., Reischl, G., Bauer, H., Leder, K., Puxbaum, H., 2012. Activation of "synthetic ambient" aerosols – relation to chemical composition of particles < 100 nm. Atmos. Environ. 54, 583–591.
Carrico, C.M., Petters, M.D., Kreidenweis, S.M., Sullivan, A.P., McMeeking, G.R., Levin, E.J.T., Engling, G., Malm, W.C., Collett Jr., J.L., 2010. Water uptake and chemical composition of fresh aerosols generated in open burning of biomass. Atmos. Chem. Phys. 10, 5165–5178.
Cerully, K.M., Raatikainen, T., Lance, S., Tkacik, D., Tiitta, P., Petaja, T., Ehn, M., Kulmala, M., Worsnop, D.R., LaaksonenA, Smith J.N., Nenes, A., 2011. Aerosol hygroscopicity and CCN activation kinetics in a boreal forest environment during the 2007 EUCAARI campaign. Atmos. Chem. Phys. 11, 12369–12386.
Chang, R.Y.W., Slowik, J.G., Shantz, N.C., Vlasenko, A., Liggio, J., Sjostedt, S.J., Leaitch, W.R., Abbatt, J.P.D., 2010. The hygroscopicity parameter (κ) of ambient organic aerosol at a field site subject to biogenic and anthropogenic influences: relationship to degree of aerosol oxidation. Atmos. Chem. Phys. 10, 5047–5064.
Dey, S., Tripathi, S.N., 2008. Aerosol direct radiative effects over Kanpur in the Indo-Gangetic basin, northern India: long-term (2001–2005) observations and implications to regional climate. J. Geophys. Res. 113, D04212.
Draxler, R.R., Hess, G.D., 1997. Description of the HYSPLIT_4 Modeling System. NOAA Tech. 405 Memo. ERL ARL-224. NOAA Air Resources Laboratory, Silver Spring, MD, p. 24.
Dusek, U., Frank, G.P., Hildebrandt, L., Curtius, J., Schneider, J., Walter, S., Chand, D., Drewnick, F., Hings, S., Jung, D., Borrmann, S., Andreae, M.O., 2006. Size matters more than chemistry for cloud-nucleating ability of aerosol particles. Science 312, 1375–1378.
Ervens, B., Feingold, G., Kreidenweis, S.M., 2005. Influence of water-soluble organic carbon on cloud drop number concentration. J. Geophys. Res. 110.
Fors, E.O., Swietlicki, E., Svenningsson, B., Kristensson, A., Frank, G.P., Sporre, M., 2011. Hygroscopic properties of the ambient aerosol in southern Sweden – a two year study. Atmos. Chem. Phys. 11, 8343–8361.
Frank, G.P., Dusek, U., Andreae, M.O., 2006. Technical note: a method for measuring size-resolved CCN in the atmosphere. Atmos. Chem. Phys. Discuss. 6, 4879–4895.
Gunthe, S.S., King, S.M., Rose, D., Chen, Q., Roldin, P., Farmer, D.K., Jimenez, J.L., Artaxo, P., Andreae, M.O., Martin, S.T., Poschl, U., 2009. Cloud condensation nuclei in pristine tropical rainforest air of Amazonia: size-resolved measurements and modeling of atmospheric aerosol composition and CCN activity. Atmos. Chem. Phys. 9, 7551–7575.
Gunthe, S.S., Rose, D., Su, H., Garland, R.M., Achtert, P., Nowak, A., Wiedensohler, A., Kuwata, M., Takegawa, N., Kondo, Y., Hu, M., Shao, M., Zhu, T., Andreae, M.O., Pöschl, U., 2011. Cloud condensation nuclei (CCN) from fresh and aged air pollution in the megacity region of Beijing. Atmos. Chem. Phys. 11, 11023–11039.
Hudson, J.G., Yum, S.S., 2002. Cloud condensation nuclei spectra and polluted and clean clouds over the Indian Ocean. J. Geophys. Res. 107, 12.
IPCC, Solomon, S., Qin, D., Manning, M., Marquis, M., Averyt, K., Tignor, M.M.B., Miller, H.L.J., Chen, Z. (Eds.), 2007. Climate Change 2007 – the Physical Science Basis. Contribution of Working Group I to the Fourth Assessment Report of the Inter-governmental Panel on Climate Change. Cambridge University Press, Cambridge, pp. 153-154–171-172.
Jai Devi, J., Tripathi, S.N., Gupta, T., Singh, B.N., Gopalakrishnan, V., Dey, S., 2011. Observation-based 3-D view of aerosol radiative properties over Indian Continental Tropical Convergence Zone: implications to regional climate. Tellus B 63, 971–989.
Jurányi, Z., Gysel, M., Weingartner, E., DeCarlo, P.F., Kammermann, L., Baltensperger, U., 2010. Measured and modelled cloud condensation nuclei

number concentration at the high alpine site Jungfraujoch. Atmos. Chem. Phys. 10, 7891–7906.
Jurányi, Z., Gysel, M., Weingartner, E., Bukowiecki, N., Kammermann, L., Baltensperger, U., 2011. A 17 month climatology of the cloud condensation nuclei number concentration at the high alpine site Jungfraujoch. J. Geophys. Res. 116.
Kammermann, L., Gysel, M., Weingartner, E., Baltensperger, U., 2010. 13-month climatology of the aerosol hygroscopicity at the free tropospheric site Jungfraujoch (3580 m a.s.l.). Atmos. Chem. Phys. 10, 10717–10732.
Kanawade, V.P., Bhattu, Deepika, Tripathi, S.N., 2014. Sub-micron Particle Number-size Distributions Characteristics at an Urban Location, Kanpur, in the Indo-Gangetic Plain (in preparation).
Kim, J.H., Yum, S.S., Shim, S., Yoon, S.C., Hudson, J.G., Park, J., Lee, S.J., 2011. On aerosol hygroscopicity, cloud condensation nuclei (CCN) spectra and critical supersaturation measured at two remote islands of Korea between 2006 and 2009. Atmos. Chem. Phys. 11, 12627–12645.
King, S.M., Rosenoern, T., Shilling, J.E., Chen, Q., Wang, Z., Biskos, G., McKinney, K.A., Pöschl, U., Martin, S.T., 2010. Cloud droplet activation of mixed organic-sulfate particles produced by the photooxidation of isoprene. Atmos. Chem. Phys. Discuss. 10, 213–244.
Kulmala, M., Kerminen, V.M., Anttila, T., Laaksonen, A., O'Dowd, C.D., 2004. Organic aerosol formation via sulphate cluster activation. J. Geophys. Res. 109.
Lance, S., Raatikainen, T., Onasch, T., Worsnop, D.R., Yu, X.Y., Alexander, M.L., Stolzenburg, M.R., McMurry, P.H., Smith, J.N., Nenes, A., 2012. Aerosol mixing-state, hygroscopic growth and cloud activation efficiency during MIRAGE 2006. Atmos. Chem. Phys. Discuss. 12, 15709–15742.
Lathem, T.L., Nenes, A., 2011. Water vapor depletion in the DMT continuous-flow CCN chamber: effects on supersaturation and droplet growth. Aerosol Sci. Technol. 45, 604–615.
Levin, E.J.T., Prenni, A.J., Petters, M.D., Kreidenweis, S.M., Sullivan, R.C., Atwood, S.A., Ortega, J., DeMott, P.J., Smith, J.N., 2012. An annual cycle of size-resolved aerosol hygroscopicity at a forested site in Colorado. J. Geophys. Res. 117, D06201.
Liu, X., Wang, J., 2010. How important is organic aerosol hygroscopicity to aerosol indirect forcing? Environ. Res. Lett. 5, 044010.
Lohmann, U., Feichter, J., 2005. Global indirect aerosol effects: a review. Atmos. Chem. Phys. 5, 715–737.
Massoli, P., Lambe, A.T., Ahern, A.T., Williams, L.R., Ehn, M., Mikkilä, J., Canagaratna, M.R., Brune, W.H., Onasch, T.B., Jayne, J.T., Petäjä, T., Kulmala, M., Laaksonen, A., Kolb, C.E., Davidovits, P., Worsnop, D.R., 2010. Relationship between aerosol oxidation level and hygroscopic properties of laboratory generated secondary organic aerosol (SOA) particles. Geophys. Res. Lett. 37, L24801.
Mishra, S.K., Dey, S., Tripathi, S.N., 2008. Implications of particle composition and shape to dust radiative effect: a case study from the Great Indian Desert. Geophys. Res. Lett. 35, L23814.
Mochida, M., Nishita-Hara, C., Kitamori, Y., Aggarwal, S.G., Kawamura, K., Miura, K., Takami, A., 2010. Size-segregated measurements of cloud condensation nucleus activity and hygroscopic growth for aerosols at Cape Hedo, Japan, in spring 2008. J. Geophys. Res. 115.
Moore, R.H., Bahreini, R., Brock, C.A., Froyd, K.D., Cozic, J., Holloway, J.S., Middlebrook, A.M., Murphy, D.M., Nenes, A., 2011. Hygroscopicity and composition of Alaskan Arctic CCN during April 2008. Atmos. Chem. Phys. 11, 11807–11825.
Moore, R.H., Karydis, V.A., Capps, S.L., Lathem, T.L., Nenes, A., 2012. Droplet number prediction uncertainties from CCN: an integrated assessment using observations and a global adjoint model. Atmos. Chem. Phys. Discuss. 12, 20483–20517.
Padró, L.T., Moore, R.H., Zhang, X., Rastogi, N., Weber, R.J., Nenes, A., 2012. Mixing state and compositional effects on CCN activity and droplet growth kinetics of size-resolved CCN in an urban environment. Atmos. Chem. Phys. 12, 10239–10255.
Patidar, V., Tripathi, S.N., Bharti, P.K., Gupta, T., 2012. First surface measurement of cloud condensation nuclei over Kanpur, IGP: role of long range transport. Aerosol Sci. Technol. 46, 973–982.
Petters, M.D., Carrico, C.M., Kreidenweis, S.M., Prenni, A.J., DeMott, P.J., Collett, J.L., Moosmüller, H., 2009. Cloud condensation nucleation activity of biomass burning aerosol. J. Geophys. Res. 114.
Petters, M.D., Kreidenweis, S.M., 2007. A single parameter representation of hygroscopic growth and cloud condensation nucleus activity. Atmos. Chem. Phys. 7, 1961–1971.
Pruppacher, H.R., Klett, J.D., 1997. Microphysics of Clouds and Precipitation. Kluwer Academic Publishers, Dordrecht, pp. 288–289.
Ram, K., Sarin, M.M., Tripathi, S.N., 2010. A 1 year record of carbonaceous aerosols from an urban site in the Indo-Gangetic Plain: characterization, sources, and temporal variability. J. Geophys. Res. 115, D24313.
Ram, K., Sarin, M.M., Tripathi, S.N., 2012. Temporal trends in atmospheric $PM_{2.5}$, PM_{10}, elemental carbon, organic carbon, water-soluble organic carbon, and optical properties: impact of biomass burning emissions in the Indo-Gangetic Plain. Environ. Sci. Technol. 46 (2), 686–695.
Rissler, J., Swietlicki, E., Zhou, J., Roberts, G., Andreae, M.O., Gatti, L.V., Artaxo, P., 2004. Physical properties of the sub-micrometer aerosol over the Amazon rain forest during the wet-to-dry season transition – comparison of modeled and measured CCN concentrations. Atmos. Chem. Phys. 4, 2119–2143.
Rissman, T.A., Varutbangkul, V., Surratt, J.D., Topping, D.O., McFiggans, G., Flagan, R.C., Seinfeld, J.H., 2007. Cloud condensation nucleus (CCN) behavior of organic aerosol particles generated by atomization of water and methanol solutions. Atmos. Chem. Phys. 7, 2949–2971.
Roberts, G.C., Nenes, A., 2005. Continuous flow streamwise thermal-gradient CCN chamber for atmospheric measurements. Aerosol Sci. Technol. 39 (3), 206–221.
Rose, D., Gunthe, S.S., Mikhailov, E., Frank, G.P., Dusek, U., Andreae, M.O., Pöschl, U., 2008. Calibration and measurement uncertainties of a continuous-flow cloud condensation nuclei counter (DMT-CCNC): CCN activation of ammonium sulfate and sodium chloride aerosol particles in theory and experiment. Atmos. Chem. Phys. 8, 1153–1179.
Rose, D., Nowak, A., Achtert, P., Wiedensohler, A., Hu, M., Shao, M., Zhang, Y., Andreae, M.O., Poschl, U., 2010. Cloud condensation nuclei in polluted air and biomass burning smoke near the mega-city Guangzhou, China – part 1: size-resolved measurements and implications for the modeling of aerosol particle hygroscopicity and CCN activity. Atmos. Chem. Phys. 10, 3365–3383.
Rosenfeld, D., Lohmann, U., Raga, G.B., O'Dowd, C.D., Kulmala, M., Fuzzi, S., Reissell, A., Andreae, M.O., 2008. Flood or drought: how do aerosols affect precipitation? Science 321, 1309–1313.
Ruehl, C.R., Chuang, P.Y., Nenes, A., 2008. How quickly do cloud droplets form on atmospheric particles? Atmos. Chem. Phys. 8, 1043–1055.
Sihto, S.L., Mikkilä, J., Vanhanen, J., Ehn, M., Liao, L., Lehtipalo, K., Aalto, P.P., Duplissy, J., Petäjä, T., Kerminen, V.M., Boy, M., Kulmala, M., 2011. Seasonal variation of CCN concentrations and aerosol activation properties in boreal forest. Atmos. Chem. Phys. 11, 13269–13285.
Srivastava, M., Tripathi, S.N., Dwivedi, A.K., Dalai, R., Bhattu, D., Bharti, P.K., Jaidevi, J., Gupta, T., 2013. CCN closure results from Indian Continental Tropical Convergence Zone (CTCZ) aircraft experiment. Atmos. Res. 132-133, 322–331.
Tritscher, T., Dommen, J., DeCarlo, P.F., Gysel, M., Barmet, P.B., Praplan, A.P., Weingartner, E., Prévôt, A.S.H., Riipinen, I., Donahue, N.M., Baltensperger, U., 2011. Volatility and hygroscopicity of aging secondary organic aerosol in a smog chamber. Atmos. Chem. Phys. 11, 11477–11496.
Twomey, S., 1974. Pollution and the planetary albedo. Atmos. Environ. 8, 1251–1256.
Vestin, A., Rissler, J., Swietlicki, E., Frank, G.P., Andreae, M.O., 2007. Cloud-nucleating properties of the Amazonian biomass burning aerosol: cloud condensation nuclei measurements and modeling. J. Geophys. Res. 112, D14201.
Zhang, Q.A., Quan, J.N., Tie, X.X., Huang, M.Y., Ma, X.C., 2011. Impact of aerosol particles on cloud formation: aircraft measurements in China. Atmos. Environ. 45, 665–672.